Molecular Cell
Article

Control of Macroautophagy by Calcium, Calmodulin-Dependent Kinase Kinase-β, and Bcl-2

Maria Høyer-Hansen,[1] Lone Bastholm,[2] Piotr Szyniarowski,[1] Michelangelo Campanella,[3] György Szabadkai,[3,4] Thomas Farkas,[1] Katiuscia Bianchi,[3,4] Nicole Fehrenbacher,[1] Folmer Elling,[2] Rosario Rizzuto,[3] Ida Stenfeldt Mathiasen,[1,5] and Marja Jäättelä[1,*]

[1] Apoptosis Department and Centre for Genotoxic Stress Research, Institute of Cancer Biology, Danish Cancer Society, 2100 Copenhagen, Denmark
[2] Institute of Molecular Pathology, Faculty of Health Sciences, University of Copenhagen, 2100 Copenhagen, Denmark
[3] Department of Experimental and Diagnostic Medicine, Section of General Pathology, University of Ferrara, 44100 Ferrara, Italy
[4] INSERM U 807, Necker Faculty, Paris V University, 75015 Paris, France
[5] Present address: Cancer and Immunobiology, Novo Nordisk A/S, DK-2760 Måløv, Denmark.
*Correspondence: mj@cancer.dk
DOI 10.1016/j.molcel.2006.12.009

SUMMARY

Macroautophagy is an evolutionary conserved lysosomal pathway involved in the turnover of cellular macromolecules and organelles. In spite of its essential role in tissue homeostasis, the molecular mechanisms regulating mammalian macroautophagy are poorly understood. Here, we demonstrate that a rise in the free cytosolic calcium ($[Ca^{2+}]_c$) is a potent inducer of macroautophagy. Various Ca^{2+} mobilizing agents (vitamin D_3 compounds, ionomycin, ATP, and thapsigargin) inhibit the activity of mammalian target of rapamycin, a negative regulator of macroautophagy, and induce massive accumulation of autophagosomes in a Beclin 1- and Atg7-dependent manner. This process is mediated by Ca^{2+}/calmodulin-dependent kinase kinase-β and AMP-activated protein kinase and inhibited by ectopic Bcl-2 located in the endoplasmatic reticulum (ER), where it lowers the $[Ca^{2+}]_{ER}$ and attenuates agonist-induced Ca^{2+} fluxes. Thus, an increase in the $[Ca^{2+}]_c$ serves as a potent inducer of macroautophagy and as a target for the antiautophagy action of ER-located Bcl-2.

INTRODUCTION

Cellular homeostasis is dependent on the balance between the biosynthesis and degradation of its components. Macroautophagy (here referred to as autophagy) is an evolutionary conserved lysosomal pathway involved in the turnover of long-lived proteins, other cellular macromolecules, and whole organelles (Codogno and Meijer, 2005; Kroemer and Jäättelä, 2005; Levine and Klionsky, 2004). It begins when a flat membrane cistern wraps around cytoplasmic organelles and/or a portion of cytosol, thus forming a closed double-membrane-surrounded vacuole, the autophagosome that matures in a stepwise process involving fusion events with endolysosomal vesicles. The final degradation step takes place within autolysosomes, where lysosomal hydrolases digest the luminal content of the autophagic vacuole to recyclable breakdown products.

Autophagy proceeds in a low basal level in most if not all cells, and it plays a crucial role in nutrient delivery, remodeling, differentiation, and removal of damaged molecules and organelles. Accordingly, its deregulation in mice leads to either embryonic or perinatal lethality or neurodegeneration and cancer (Hara et al., 2006; Komatsu et al., 2006; Qu et al., 2003; Yue et al., 2003). Starvation, growth factor deprivation, protein aggregation, numerous anticancer treatments, and various other stresses increase autophagic activity above the basal levels. During starvation stress, autophagy-mediated recycling of nutrients is essential for the maintenance of cellular amino acid and energy levels and thereby for cell survival (Lum et al., 2005; Onodera and Ohsumi, 2005). Similarly, autophagy serves a protective function during neuronal development and in neurons challenged with aggregate-prone proteins (Hara et al., 2006; Komatsu et al., 2006; Ravikumar et al., 2004). Paradoxically, autophagy is also associated with nonapoptotic type II cell death, also called autophagic degeneration (Baehrecke, 2005; Kroemer and Jäättelä, 2005; Tsujimoto and Shimizu, 2005). Even though autophagy genes act as mediators of the cell death in some experimental conditions, increasing evidence suggests that the accumulation of autophagosomes in dying cells or tissues commonly represents a failed rescue effort in response to external stress.

Autophagosome formation is mediated by a set of evolutionarily conserved autophagy-related proteins (Atg proteins) and inhibited by a serine threonine protein kinase originally recognized as a target of rapamycin and thereby named TOR (Codogno and Meijer, 2005; Klionsky et al., 2003). TOR functions as a sensor for cellular energy and amino acid levels and is negatively regulated by the AMP-activated protein kinase (AMPK) via a pathway

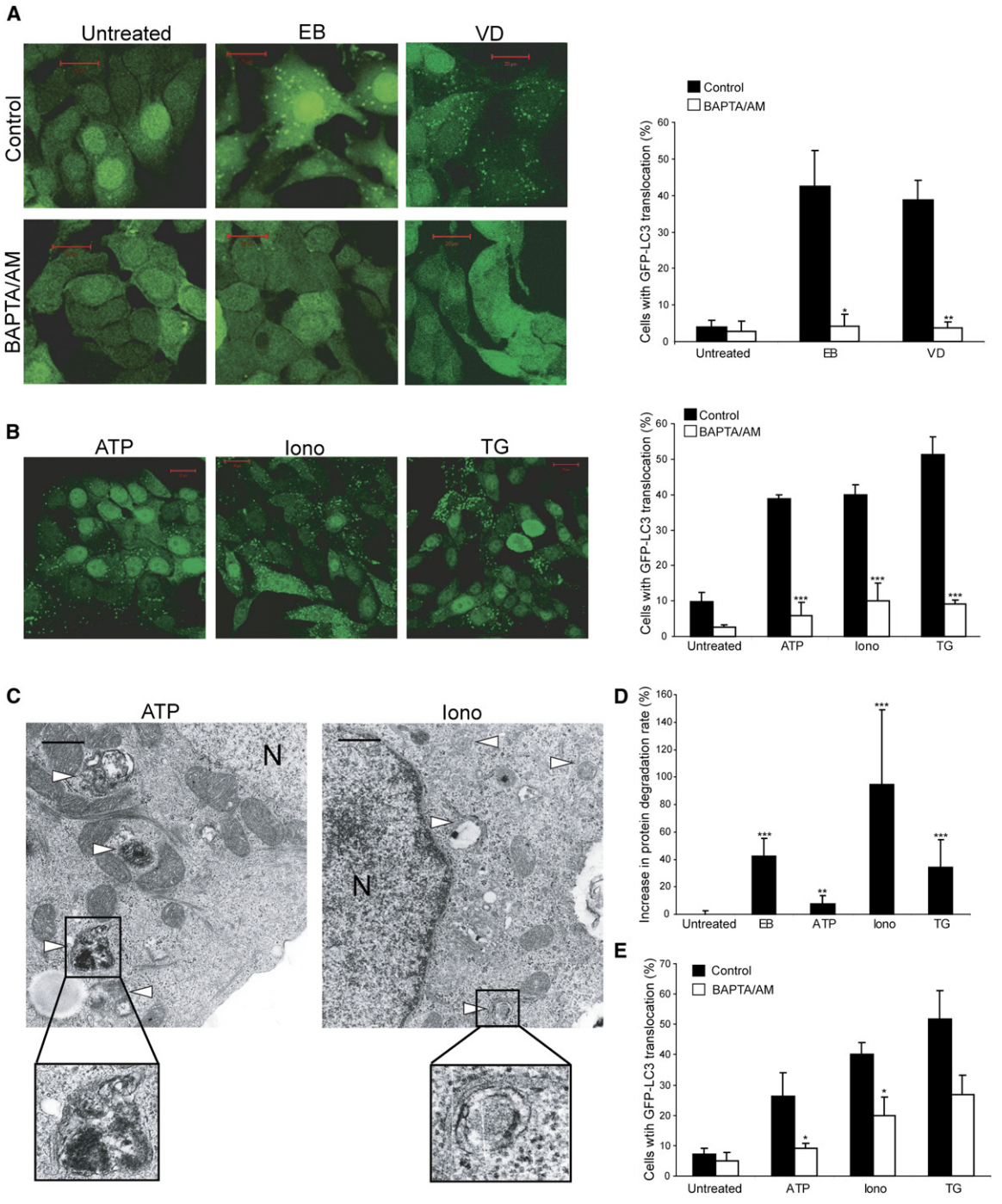

Figure 1. Ca^{2+} Is a Mediator of Autophagy

(A and B) MCF-7-eGFP-LC3 cells were left untreated (control) or treated with 100 nM EB1089 (EB) or 1,25-dihydroxyvitamin D_3 (VD) for 72 hr, 100 μM ATP for 48 hr, 10 μM ionomycin for 24 hr (Iono), or 100 nM TG for 24 hr. When indicated, 20 μM BAPTA/AM was added for the last 2 hr of the treatment. Representative confocal images (20 μm scale bars) and histograms with percentages of green cellular cross-sections with over five LC3-positive dots are shown. The values represent mean ± SD for three independent samples. Similar results were obtained in three independent experiments.

(C) Representative electron micrografs of MCF-7 cells treated with 100 μM ATP for 48 hr or 1 μM ionomycin for 24 hr. Arrows denote autophagosomes and N nulei (0.5 μm scale bars).

(D) MCF-7 cells were treated with 100 nM EB1089 or 100 μM ATP for 48 hr or with 10 μM ionomycin or 100 nM TG for 24 hr, and the increase in the degradation of long-lived proteins as compared to the untreated cultures was measured. The values represent mean ± SD for six independent duplicate experiments.

involving the GTPase activating Tuberous sclerosis complex (TSC1/2) and its substrate ras-family GTP binding protein RHEB (Sarbassov et al., 2005). AMPK can be phosphorylated and activated by LKB1 tumor suppressor kinase at low energy levels and by Ca^{2+}/calmodulin-dependent protein kinase kinase-β (CaMKK-β) in response to an increase in the cytosolic-free calcium $[Ca^{2+}]_c$ (Hawley et al., 2005; Shaw et al., 2004; Woods et al., 2005). Even though the AMPK-mediated inhibition of mammalian TOR (mTOR) has been fairly well established, direct evidence for its ability to induce autophagy is still lacking in mammalian cells. Snf1, the yeast ortholog of AMPK, has, however, been identified as a positive regulator of autophagy (Wang et al., 2001).

Beclin 1, the mammalian ortholog of yeast Atg6, represents an interesting link between autophagic and apoptotic machineries (Levine and Klionsky, 2004). Beclin 1 is a Bcl-2 interacting protein that promotes autophagosome formation when in complex with class III phosphatidylinositol-3-kinase (PI3K) and p150 myristylated kinase, whereas the Beclin 1-Bcl-2 complex functions as a brake of autophagy and autophagic cell death (Pattingre et al., 2005). Intriguingly, the autophagy inhibition by Bcl-2 is evident only when Bcl-2 resides in the ER, where it has been suggested to regulate cellular Ca^{2+} homeostasis (Ferrari et al., 2002; Oakes et al., 2006). It should be noted that Bcl-2 and the proapoptotic Bcl-2 proteins (BAX and BAK) have also been reported to enhance and inhibit the autophagic response, respectively (Lum et al., 2005; Shimizu et al., 2004). Thus, the impact of Bcl-2-like proteins on autophagy requires further exploration.

A rise in the $[Ca^{2+}]_c$ triggers disparate responses such as changes in cell metabolism, muscle contraction, neurotransmitter release, cell proliferation, and cell death (Ferrari et al., 2002). Hitherto, practically nothing is known about the role of Ca^{2+} in autophagosome formation. Prompted by the ability of the Ca^{2+}-activated CaMKK-β to activate the putative autophagy inducer AMPK, and the requirement of ER location for the antiautophagy function of Bcl-2, we investigated the role of Ca^{2+} in autophagy signaling in more detail. Using state-of-the-art methods to detect autophagy and subcellular Ca^{2+} levels, we show that Ca^{2+} regulates autophagy via a signaling pathway involving CaMKK-β, AMPK, and mTOR and that ER-located Bcl-2 effectively inhibits this pathway. Because both the CaMKK-AMPK signaling pathway and autophagy are essential for eukaryotic cells from unicellular yeast to complex tissues such as brain, these data are likely to have broad implications for our understanding of autophagy-mediated regulation of cellular homeostasis and cell survival in general.

RESULTS

An Increase in the $[Ca^{2+}]_c$ Triggers Autophagy

The active form of vitamin D_3 (1,25-dihydroxyvitamin D_3) and its chemotherapeutic analog EB1089 induce a slow increase in the $[Ca^{2+}]_c$ and autophagy followed by autophagy-dependent cell death in MCF-7 breast cancer cells (Høyer-Hansen et al., 2005; Mathiasen et al., 2002). In order to test whether the increase in the $[Ca^{2+}]_c$ actually serves as a mediator of the autophagic response, we studied the autophagosome formation in MCF-7 cells expressing the autophagosome-associated LC3 protein fused to the enhanced green fluorescence protein (eGFP-LC3). As expected, a three-day treatment of the cells with 100 nM 1,25-dihydroxyvitamin D_3 or EB1089 significantly increased the number of the cells with autophagosomes (LC3-positive vesicles; Figure 1A). Remarkably, the addition of an intracellular Ca^{2+} chelator bis-(o-aminophenoxy)-ethane-N,N,N,N′-tetraacetic acid/tetra(acetoxymethyl)-ester (BAPTA/AM) to the cells for the last 2 hr of the treatment completely abolished the autophagosomes. Thus, Ca^{2+} is required for the formation of autophagosomes in response to vitamin D_3 compounds, whereas their turnover by the fusion with the lysosomal vesicles (i.e., the disappearance of the LC3-positive vesicles) appears to be Ca^{2+} independent.

Prompted by the ability of BAPTA/AM to inhibit 1,25-dihydroxyvitamin D_3- and EB1089-induced autophagosome formation, we next investigated whether an increase in the $[Ca^{2+}]_c$ is enough to trigger autophagy. For this purpose, we treated the eGFP-LC3 expressing MCF-7 cells with three stimuli that increase the $[Ca^{2+}]_c$ by different means: (1) ATP that acts on P2 purinoreceptors to generate inositol 1,4,5-triphosphate (IP_3) that triggers the release of Ca^{2+} from the ER through IP_3 receptor-regulated channels, (2) ionomycin, a Ca^{2+} ionophore that serves as a mobile Ca^{2+} carrier that equilibrates Ca^{2+} levels across biological membranes, including plasma and ER membranes, and (3) thapsigargin (TG), an inhibitor of ER Ca^{2+}-ATPase (Dixon et al., 1997; Ferrari et al., 2002; Kao, 1994). All treatments induced a significant increase in the number of cells with LC3-positive vesicles, and in all cases, the effect was effectively inhibited by BAPTA/AM (Figure 1B). Transmission electron microscopy (EM) ensured that the induction of LC3-postive vesicles by all three Ca^{2+} mobilizing agents correlated with the formation of autophagosomes, cytosolic vesicles surrounded by a double membrane (Figure 1C and data not shown). Importantly, all the Ca^{2+} mobilizing agents also enhanced the degradation of long-lived proteins, indicating that the morphological changes observed by confocal microscopy

(E) HeLa cells transiently transfected with eGFP-LC3 were treated with 100 μM ATP, 10 μM ionomycin, or 100 nM TG for 24 hr, and percentages of green cross-sections with over five LC3-positive dots were counted. When indicated, the treatment was followed by 1 hr incubation with 10 μM BAPTA/AM. The values represent mean ± SD for three independent samples. Similar results were obtained in two independent experiments.
*p value < 0.05, **p value < 0.01, and ***p value < 0.001 as compared to control samples without BAPTA/AM (A, B, and E) or untreated cells (D).

and transmission EM reflected functional autophagy (Figure 1D). Furthermore, Ca^{2+} mobilizing agents induced BAPTA/AM-sensitive autophagosome formation in HeLa cervix carcinoma cells (Figure 1E). Consistent with the more potent autophagy inducing activity of TG as compared with ATP, 24 hr treatment of MCF-7 cells with 100 nM TG and 100 μM ATP reduced the $[Ca^{2+}]_{ER}$ by 87% and 39%, respectively (data not shown). It should also be noted that ATP did not have any effect on cell growth or survival during a 5 day follow-up period, whereas TG, ionomycin, and vitamin D compounds induced cell death 1–2 days after the appearance of autophagosomes (Høyer-Hansen et al., 2005) (data not shown).

Ca^{2+}-Induced Autophagy Is Dependent on Atg Genes and CaMKK-β

Beclin 1, Atg7, and class III PI3K are required for the starvation-induced autophagosome formation. In order to test whether the Ca^{2+}-mediated autophagy proceeded by the same signaling pathway, we depleted MCF-7 cells for Beclin 1 and Atg7 by small interfering RNAs (siRNA) (Figures 2A and 2B) or treated them with 3-methyladenine (3-MA), an inhibitor of class III PI3K (Figure 2C). All treatments significantly inhibited the appearance of LC3-positive vesicles induced by EB1089, ATP, ionomycin, and TG (Figures 2B and 2C). Furthermore, autophagy induced by Ca^{2+} mobilizing agents was associated with the inhibition mTOR kinase activity as judged by the reduced phosphorylation of its substrate, ribosomal protein S6 kinase 1 ($p70^{S6K}$) in MCF-7 cells, and in immortalized murine embryonic fibroblasts (Figures 2D and 2E).

In order to gain insight into the Ca^{2+}-induced signaling pathway mediating mTOR inhibition and autophagy induction, we next tested whether the recently reported Ca^{2+}-CaMKK-β-AMPK pathway was involved in this process (Hawley et al., 2005; Woods et al., 2005). For this purpose, we first treated the cells with a CaMKK-α/β inhibitor (STO-609) (Tokumitsu et al., 2002). As demonstrated earlier in ionomycin-treated HeLa cells (Woods et al., 2005), Ca^{2+} mobilizing agents activated AMPK in an STO-609-sensitive manner in MCF-7 cells (Figure 3A). Remarkably, the STO-609-mediated inhibition of Ca^{2+}-induced AMPK activation was accompanied by a significant inhibition of autophagy in MCF-7 cells and in nontransformed MCF-10A breast epithelial cells (Figures 3B–3D). These data suggest that CaMKK and AMPK, indeed, mediate Ca^{2+}-induced autophagy. Accordingly, the inhibition of AMPK either by CaMKK-β-specific siRNA or by a pharmacological inhibitor (compound C) attenuated autophagy induced by Ca^{2+}-mobilizing agents in MCF-7 cells (Figures 3E–3H). Importantly, STO-609 and CaMKK-β siRNA also inhibited the activation of AMPK and the formation of autophagosomes in HeLa cervix carcinoma cells treated with Ca^{2+}-mobilizing agents (Figure S1 in the Supplemental Data available with this article online).

ER-Localized Bcl-2 Inhibits EB1089- and ATP-Induced Autophagy

Bcl-2 has been reported to regulate the cellular Ca^{2+} handling and to inhibit starvation-induced autophagy (Ferrari et al., 2002; Pattingre et al., 2005). Thus, we speculated that Bcl-2 could inhibit autophagy via its effects on Ca^{2+} homeostasis. In order to test this hypothesis, we expressed wild-type Bcl-2 (Bcl-2) and its mutants in which the carboxy-terminal hydrophobic sequence has been either removed (Bcl-cyt), resulting in cytosolic expression, or exchanged to a corresponding membrane anchor from an ER-specific isoform of cytochrome b5 (Bcl-ER) or *L. monocytogenes* ActA (Bcl-mito), resulting in a subcellular localization restricted to the ER and mitochondria, respectively (Zhu et al., 1996). Western blot analysis and the ability to inhibit tumor necrosis factor (TNF)-induced DNA fragmentation and cell death confirmed the equal expression levels and the functionality of the Bcl-2 chimeras, and the confocal microscopy verified their expected subcellular location in MCF-7 cells (Figure 4). Only cells expressing Bcl-ER or wild-type Bcl-2 showed colocalization with an ER marker protein, sarcoplasmic reticulum Ca^{2+}-ATPase (SERCA). Similarly, only Bcl-mito and wild-type Bcl-2 showed colocalization with the mitochondrial marker protein cytochrome *c*.

Next, we investigated the impact of Bcl-2 chimeras on Ca^{2+}-mediated autophagy by transmission EM. As we have shown earlier in the parental MCF-7 cells (Høyer-Hansen et al., 2005), a 5 day treatment of the mock-transfected cells with 100 nM EB1089 induced a massive accumulation of autophagic vacuoles surrounded by a double membrane (Figures 5A and 5B). Most of the vacuoles contained cristae-like structures resembling mitochondria, and the cross-sections of affected cells contained practically no normal mitochondria. Neither the number of cellular cross-sections with EB1089-induced autophagic vacuoles nor the appearance of the vacuoles was affected by the ectopic expression of wild-type Bcl-2, Bcl-cyt, or Bcl-mito, whereas the cross-sections of EB1089-treated Bcl-ER expressing cells were nearly devoid of autophagic structures (Figures 5A and 5B). Accordingly, only Bcl-ER was able to inhibit the EB1089-induced autophagosome formation as assessed by the translocation of eGFP-LC3 into vesicular structures (Figure S2). Akin to EB1089 treatment, Bcl-ER, but not Bcl-mito, effectively inhibited autophagy in response to ATP, whose Ca^{2+} mobilizing activity depends on ER Ca^{2+} stores (Figure 5C). On the contrary, the autophagosome formation induced by ionomycin that triggers Ca^{2+} fluxes from both the ER and the extracellular space was resistant to Bcl-2 whether localized to ER or mitochondrial membranes (Figure 5C).

ER-Localized Bcl-2 Lowers the $[Ca^{2+}]_{ER}$ and Reduces Agonist-Induced Leak of Ca^{2+} from the ER

Indirect evidence suggests that the EB1089-induced increase in the $[Ca^{2+}]_c$ originates from the ER (Mathiasen et al., 2002). In order to test whether EB1089 renders the

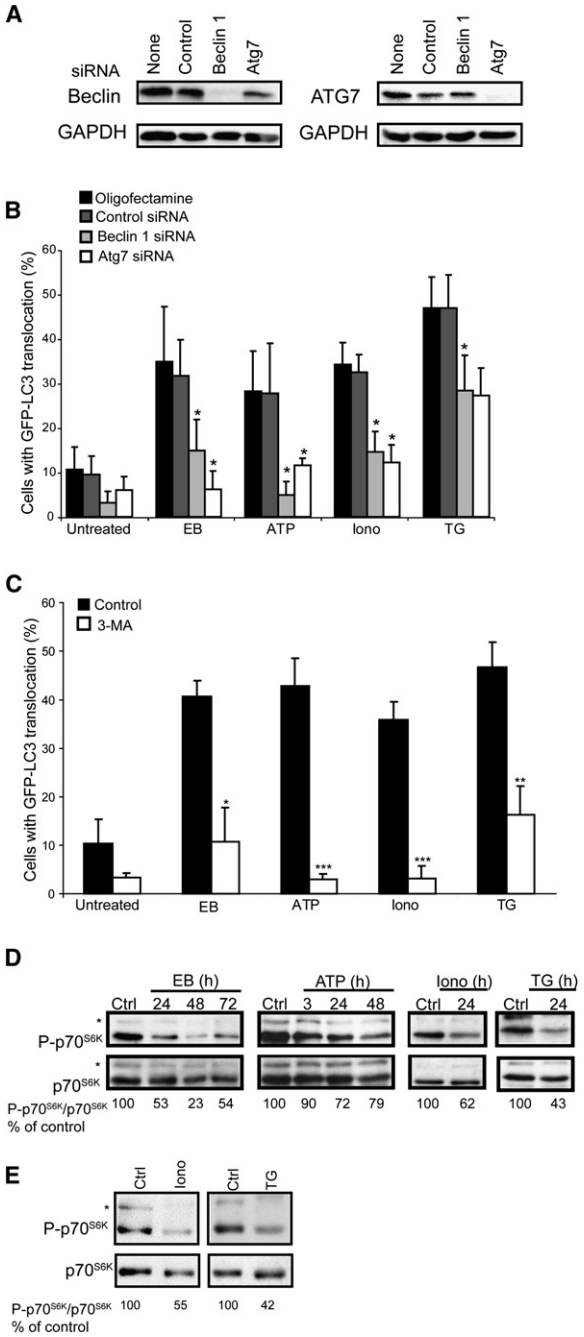

Figure 2. Involvement of ATG Genes, Class III PI3K, and mTOR in Ca^{2+}-Mediated Autophagy

(A) Immunoblot analysis of Beclin 1, Atg7, and glyceraldehyde-3-phosphate dehydrogenase (GAPDH; loading control) in MCF-7-EGFP-LC3 cells treated with oligofectamine alone or together with control, Beclin 1 or ATG7-specific siRNA 72 hr earlier.

(B) The cells (see [A]) were left untreated or treated with 100 nM EB1089 for 72 hr (EB), 100 μM ATP for 48 hr, or 10 μM ionomycin (iono) or 100 nM TG for 24 hr and analyzed for autophagosome formation 3 days after the siRNA treatment. Percentages of green cellular cross-sections with over five LC3-positive dots are shown. The values represent mean ± SD for combined data from three to five independent experiments.

(C) MCF-7-EGFP-LC3 cells were treated with the indicated Ca^{2+}-mobilizing agents and analyzed as in (B). When indicated, 10 mM 3-MA was added for the last 48 hr (EB and ATP) or 24 hr (iono and TG) of the treatment. The values represent mean ± SD for three independent samples. Similar results were obtained in three independent experiments.

(D) Proteins from MCF-7 cells left untreated (ctrl) or treated with 100 nM EB, 100 μM ATP, 10 μM ionomycin, or 100 nM TG for indicated times were analyzed by immunoblotting for the phosphorylated $p70^{S6K}$ ($P\text{-}p70^{S6K}$) and total $p70^{S6K}$ (loading control). The asterisk (*) denotes the phosphorylated (top) and total (bottom) $p85^{S6K}$ recognized by the antibodies. The values indicate the $P\text{-}p70^{S6K}$:$p70^{S6K}$ ratio as percentages of that in control cells. Similar results were obtained in two independent experiments.

(E) Proteins from NIH3T3 cells left untreated (ctrl) or treated with 10 μM ionomycin for 12 hr or 100 nM TG for 24 hr were analyzed as in (D).

*p value < 0.05, **p value < 0.01, and ***p value < 0.001 as compared to control siRNA- (B) or vehicle-treated (C) samples.

ER membrane more permeable to Ca^{2+}, we measured kinetic changes of $[Ca^{2+}]_c$ after the application of tert-butylhydroquinone (tBHQ), a reversible blocker of SERCA pumps. The resting $[Ca^{2+}]_c$ in fura-2-loaded cells was significantly higher after 72 hr treatment with EB1089 (Figure 6A), confirming our previous observations (Mathiasen et al., 2002). Furthermore, the $[Ca^{2+}]_c$ in the presence of tBHQ and external Ca^{2+} (1 mM) reached a lower steady state in EB1089-treated cells, proving again that the $[Ca^{2+}]_{ER}$ is reduced by the drug. Also, the velocity of $[Ca^{2+}]_c$ increase in the early phase after tBHQ addition was greatly enhanced, allowing us to conclude that the EB1089 induced reduction in the $[Ca^{2+}]_{ER}$-reflected Ca^{2+} leak from the ER rather than reduced Ca^{2+} extrusion through the plasma membrane. Moreover, we measured the effect of EB1089 on $[Ca^{2+}]_{ER}$ in MCF-7 cells transfected with ER-targeted aequorin (ER-AEQ), a Ca^{2+} reporter protein with highly selective subcellular localization (Chiesa et al., 2001). EB1089 induced a time-dependent decrease in $[Ca^{2+}]_{ER}$, reaching significance at day three when the $[Ca^{2+}]_{ER}$ had fallen from 200 ± 8.3 μM to 159 ± 12.6 μM (Figure 6B). These kinetics suggest that the increase in the $[Ca^{2+}]_c$ that we have earlier shown to occur three days after the start of the EB1089 treatment is a result of EB1089-induced Ca^{2+} release from the ER (Mathiasen et al., 2002).

Bcl-2 family proteins have been shown to regulate ER Ca^{2+} homeostasis in other cell types (Pinton and Rizzuto, 2006). Thus, we next investigated the effect of the Bcl-2 chimeras on the EB1089-induced fall in the $[Ca^{2+}]_{ER}$. As previously shown in different cell types, wild-type Bcl-2 significantly lowered steady-state $[Ca^{2+}]_{ER}$ in MCF-7 cells (Figure 6C). This effect of the antiapoptotic Bcl-2 family proteins has been shown to be the consequence of increased Ca^{2+} leak from the ER (Pinton and Rizzuto, 2006), which may follow Bcl-2-dependent phosphorylation of the IP_3 receptors in the ER (Oakes et al., 2005; White et al., 2005). These data suggest that the effect is dependent on ER-localized Bcl-2. Indeed, cells expressing Bcl-ER had a more robust decrease in steady state $[Ca^{2+}]_{ER}$ as compared to Bcl-WT transfected cells, whereas Bcl-mito

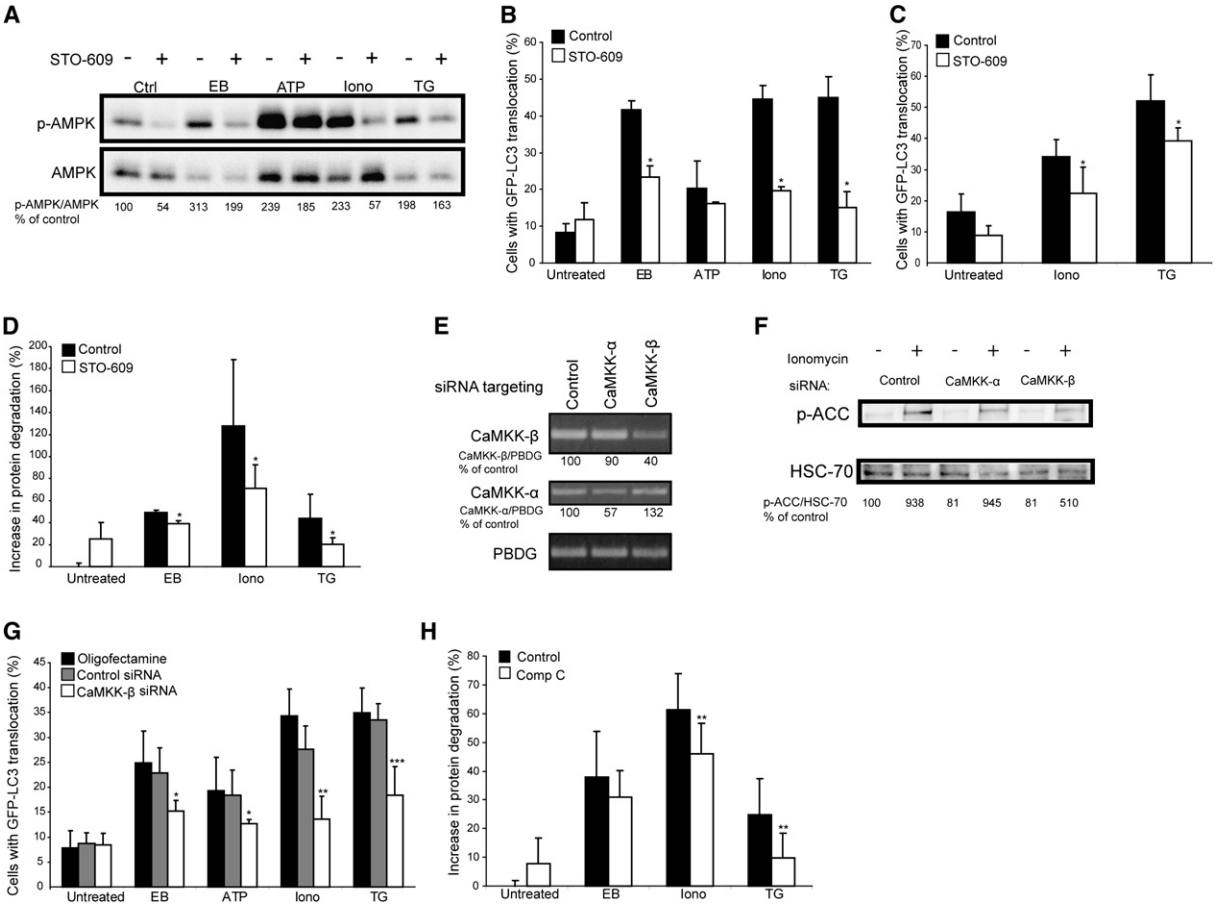

Figure 3. Ca^{2+} Activates AMPK and Induces Autophagosome Formation via CaMKK-β

(A) Proteins from MCF-7 cells left untreated (ctrl) or treated with 100 nM EB, 100 μM ATP, 10 μM ionomycin, or 100 nM TG for 24 hr were analyzed by immunobloting for p-AMPK and total AMPK expression. When indicated, 25 μM STO-609 was added for the last 12 hr. The values indicate the p-AMPK:total AMPK ratio as a percentage of that in control cells.

(B and C) MCF-7-EGFP-LC3 (B) and MCF10A-EGFP-LC3 (C) cells were left untreated or treated with the indicated drugs as in (A) with or without 25 μM STO-609 for 24 hr. Percentages of green cellular cross-sections with over five LC3-positive dots are shown. The values represent mean ± SD for one triplicate experiment.

(D) The increase in the degradation of long-lived proteins was measured in MCF-7 cells treated with 100 nM EB1089 for 48 hr or 10 μM ionomycin or 100 nM TG for 24 hr. When indicated, 25 μM STO-609 was added for the last 24 hr of the experiment. The values are expressed as percentages of untreated cells and represent mean ± SD for three independent duplicate experiments.

(E) The mRNA level of CaMKK-α, CaMKK-β, or PorphoBilinoGen Deaminase (pBGD) was analyzed by quantitative RT-PCR in MCF-7 cells 72 hr after the transfection with the indicated siRNAs.

(F) Immunoblot analysis of proteins p-ACC and HSC70 (loading control) from MCF7 cells 72 hr after the transfection with indicated siRNAs. The cells were left untreated or treated with 10 μM ionomycin for the last 24 hr. The values indicate the p-ACC:HSC70 ratios as percentages of the ratio in untreated control siRNA-transfected cells.

(G) MCF-7-EGFP-LC3 treated with oligofectamine alone or together with either control or CaMKK-β-specific siRNAs for 72 hr were left untreated or treated with 100 nM EB or 100 μM ATP for the last 48 hr or with 10 μM ionomycin or 100 nM TG for the last 24 hr. The LC3 translocation was evaluated as in (B) and (C), and the values represent mean ± SD for three independent duplicate experiments.

(H) MCF-7 cells were treated and analyzed as in (D) except for 5 μM compound C (Comp C) that was added for the last 24 hr when indicated. The values represent mean ± SD for three independent duplicate experiments.

*p value < 0.05, **p value < 0.01, and ***p value < 0.001 as compared to samples without STO-609 (B–D) or compound C (H) or with control siRNA (G).

and Bcl-cyt did not change the $[Ca^{2+}]_{ER}$ significantly (Figure 6C). Importantly, only Bcl-ER was able to inhibit the EB1089-induced partial $[Ca^{2+}]_{ER}$ depletion, whereas wild-type Bcl-2, Bcl-cyt, and Bcl-mito failed to do so (Figure 6D). Notably, Bcl-mito almost doubled the EB1089-induced decrease in the $[Ca^{2+}]_{ER}$. Importantly, Bcl-ER also inhibited the ATP-induced release of Ca^{2+} from the ER as shown by its ability to significantly inhibit both the ATP-induced decrease in the $[Ca^{2+}]_{ER}$ as well as the increase in the $[Ca^{2+}]_c$ (Figures 6E and 6F). Due to technical problems, we could not test the effect of Bcl-ER in TG-induced Ca^{2+} fluxes by this method. It should,

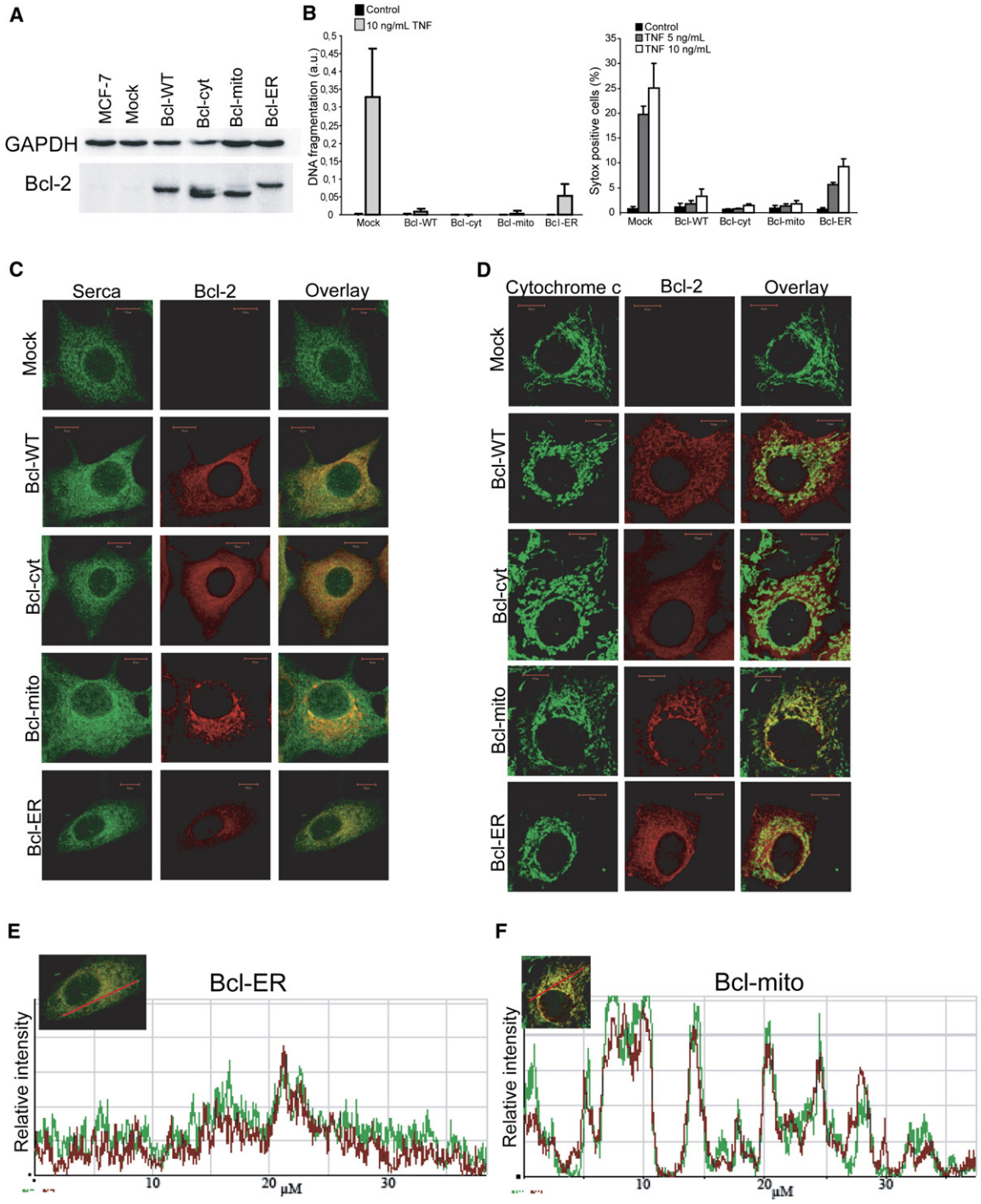

Figure 4. Characterization of MCF-7 Cells Expressing Wild-Type Bcl-2 or the Bcl-2 Chimeras with Restricted Subcellular Location

(A) Immunoblot analysis of parental MCF-7 cells and single-cell clones transfected with indicated plasmid constructs.

(B) ELISA-based analysis of apoptosis-associated DNA fragmentation (right) and uptake of Sytox as determined by FACS analysis (left) in the indicated MCF-7 transfectants left untreated (control) or treated with the indicated concentrations of TNF for 36 hr. The values represent mean ± SD for combined data from four independent duplicate experiments.

(C–F) Representative confocal images (C and D) of the indicated MCF-7 transfectants costained with antibodies to SERCA (green; [C] and [E]) or cytochrome *c* (green; [D] and [F]) and Bcl-2 (red). The profiles of relative intensities of the two fluorophores along the red line marked in the pictures were used to evaluate the colocalization (E and F).

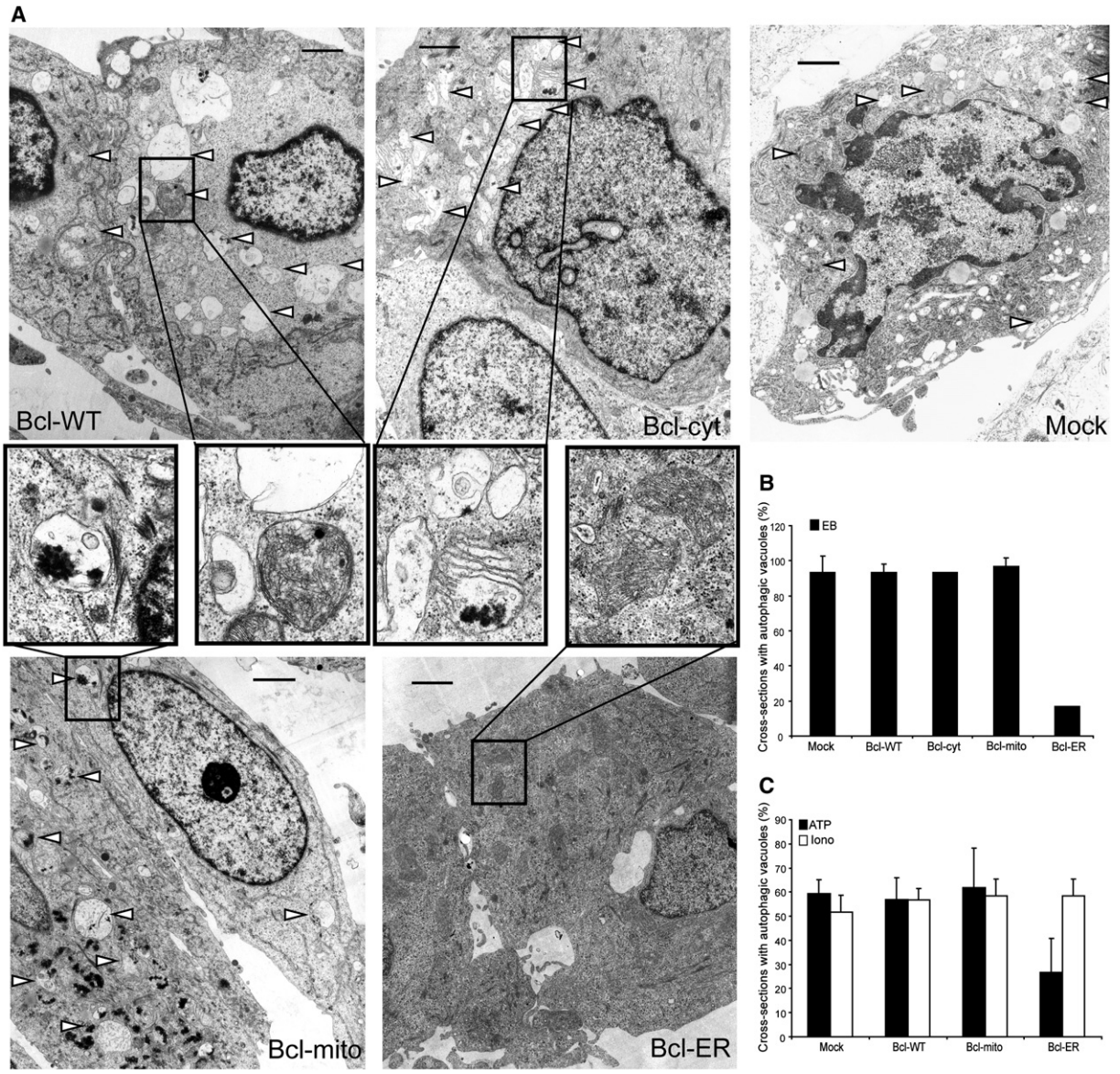

Figure 5. ER-Targeted Bcl-2 Inhibits EB1089- and ATP-Induced Autophagy

(A and B) MCF-7 cells transfected with the indicated Bcl-2 constructs were treated with 100 nM EB for 5 days before fixation for the transmission EM. The large images were taken with a 5000× objective (1 μM scale bars) and the close-up images with a 20,000× objective. Examples of autophagic vacuoles are marked with arrows. Percentages of cross-sections with autophagic vesicles were obtained by counting 30 randomly chosen cross-sections. The values represent mean ± SD for combined data from two independent experiments (Bcl-cyt was tested only once) with two independent single-cell clones.

(C) MCF-7 cells transfected with the indicated Bcl-2 constructs were treated with 100 μM ATP for 48 hr or 1 μM ionomycin for 24 hr and analyzed by transmission EM as in (A). The values represent mean ± SD for data combined from two independent blocks.

however, be noted that the decrease in the $[Ca^{2+}]_{ER}$ induced by another SERCA pump inhibitor (tBHQ) was effectively inhibited by Bcl-ER (data not shown). Thus, we conclude that Bcl-ER, either through a direct effect on the ER membrane or indirectly by reducing the steady state $[Ca^{2+}]_{ER}$ (the driving force for Ca^{2+} leak), is able to specifically inhibit agonist-induced Ca^{2+} release into the cytoplasm, which might explain its capacity to inhibit Ca^{2+}-mediated autophagosome formation.

DISCUSSION

Ca^{2+} Mobilizing Agents Trigger Autophagy

Our data demonstrate that the Ca^{2+} mobilizing agents are potent inducers of autophagy. A massive increase in the number of autophagosomes was evident following unrelated Ca^{2+} mobilizing stimuli such as (1) vitamin D compounds that induce a slow release of Ca^{2+} from the ER, (2) ATP that generates IP_3 and activates IP_3

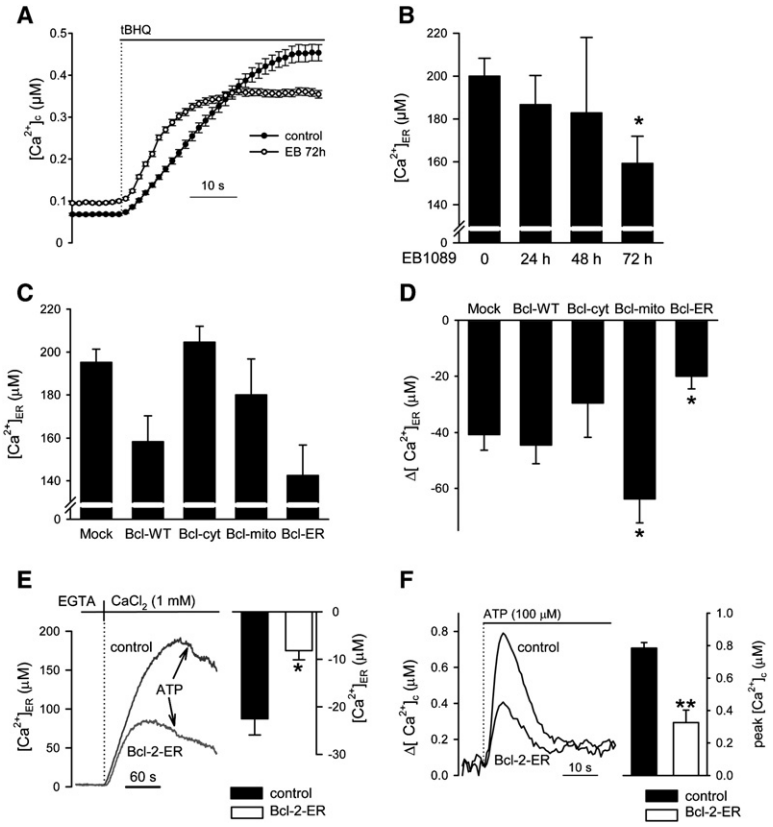

Figure 6. Bcl-ER Inhibits EB1089-Induced Calcium Fluxes

(A) For $[Ca^{2+}]_c$ measurements, fura-2-loaded MCF-7 cells were imaged as described in the Experimental Procedures. Control cells and cells treated with 100 nM EB1089 for 72 hr were stimulated with 100 μM tBHQ, as indicated. Traces were calibrated according to standard protocols (Szabadkai et al., 1999), and the mean ± SEM of >40 cells from three independent experiments is shown. Resting $[Ca^{2+}]_c$ before tBHQ addition was 66.4 ± 2.6 nM in nontreated cells versus 92.6 ± 2.7 nM after EB1089 treatment. Steady-state plateau after tBHQ addition was 408.4 ± 19.8 nM in controls versus 385.0 ± 8.6 in EB1089-treated cells.

(B) Steady-state $[Ca^{2+}]_{ER}$ was measured in MCF-7 cells transiently transfected with ER-AEQ and left untreated or treated with 100 nM EB1089 for the indicated periods. Mean ± SEM from nine experiments are shown. *$p < 0.05$.

(C) $[Ca^{2+}]_{ER}$ was measured in cells cotransfected with the ER-AEQ probe and the indicated Bcl-2 constructs and is presented as mean ± SEM from eight experiments as in (B). *$p < 0.05$.

(D) The effect of differentially targeted Bcl-2 constructs on EB1089 induced Ca^{2+} depletion. $[Ca^{2+}]_{ER}$ was measured in cells transfected as in (C) and left untreated or treated with 100 nM EB1089 for 72 hr. The effect of EB1089 was calculated from paired data from the two groups (nontreated minus EB1089 treated). Mean ± SEM of the differences ($\Delta[Ca^{2+}]_{ER}$) is shown from a minimum of nine experiments. *$p < 0.05$.

(E) Effect of Bcl-2-ER on steady-state $[Ca^{2+}]_{ER}$ and ATP-induced Ca^{2+} release. MCF-7 cells were transiently transfected with the erAEQ probe alone (control) or with Bcl-2-ER. After reconstitution of erAEQ with coelenterazine (see Experimental Procedures), cells were perfused with Ca^{2+}-free KRB solution containing 100 μM EGTA. KRB containing 1 mM $CaCl_2$ was added as indicated to induce ER Ca^{2+} uptake. After reaching the steady-state $[Ca^{2+}]_{ER}$ levels, cells were stimulated with 100 μM ATP (arrows in the left panel). The left panel shows representative traces of $[Ca^{2+}]_{ER}$ measurements from control and Bcl-2-ER-transfected cells, and the right panel shows mean ± SEM of $[Ca^{2+}]_{ER}$ changes after ATP addition from greater than seven traces from two independent experiments.

(F) Effect of Bcl-2-ER on ATP-induced Ca^{2+} release. MCF-7 cells were transiently transfected with the cytAEQ probe alone (control) or with ER Bcl-2-ER. Cells were perfused with KRB containing 1 mM $CaCl_2$ and stimulated with 100 μM ATP as indicated. The left panel shows representative traces of $[Ca^{2+}]_c$ measurements. The right panel shows mean ± SEM of $[Ca^{2+}]_c$ peaks after ATP addition from greater than seven traces from two separate experiments.

receptor-regulated Ca^{2+} channels in the ER, (3) TG that inhibits ER Ca^{2+}-ATPase, and (4) ionomycin that allows Ca^{2+} fluxes from both the extracelluar space and the ER (Ferrari et al., 2002; Kao, 1994; Mathiasen et al., 2002). Importantly, the accumulation of autophagosomes induced by all Ca^{2+} mobilizing agents was accompanied by a significant increase in the degradation rate of long-lived proteins that reflects functional autophagy. Thus, the increase in the number of autophagosomes in cells treated with Ca^{2+} mobilizing agents is due to the increased formation of autophagosomes rather than their defective turnover.

Even though the existing autophagy literature frequently lists Ca^{2+} as a putative second messenger, the experimental challenging of this hypothesis has been very limited. Consistent with our data, Seglen and coworkers have shown that calcium chelators (BAPTA/AM, EGTA, and EDTA) suppress constitutive autophagy in hepatocytes as analyzed by the sequestration of lactate dehydrogenase (LDH) into cytosolic vesicles (Gordon et al., 1993). Based on the inhibitory effect of Ca^{2+} mobilizing agents in their model system, they concluded, however, that LDH autophagy depends on intracellular Ca^{2+} stores rather than the increase in the $[Ca^{2+}]_c$. This controversy may be due to the differences in experimental set ups. First, the LDH autophagy in hepatocytes was analyzed 3 hr after the stimuli, whereas the increase in ATP-, ionomycin, TG-, and EB1089-induced autophagosome formation was first evident after a lag time of 24–72 hr. Second, the inhibitory effect of TG on LDH sequestration was detected only at micromolar concentrations, whereas the formation of autophagosomes in our model system was

evident at 100 nM. We have earlier shown that TG is an effective inducer of lysosomal membrane permeabilization (Høyer-Hansen et al., 2005), an event that could explain the autophagy inhibitory effect of high concentrations of TG. Third, the LDH sequestration assay may measure microautophagy in addition to macroautophagy analyzed in this study. Finally, BAPTA/AM, which is hydrolyzed to a membrane-impermeable form by cytosolic esterases and thereby arrested in the cytosol, inhibited autophagy in both model systems. Thus, the increased $[Ca^{2+}]_c$ rather than Ca^{2+} in other cellular compartments appears responsible for the autophagy induction. This conclusion is further supported by the identification of a cytosolic Ca^{2+}-activated kinase, CaMKK-β, as an essential mediator of Ca^{2+}-induced autophagy, as well as by the finding that inhibition of autophagy by targeted Bcl-2 constructs was related to their effect on agonist-induced Ca^{2+} release from the ER and not on the steady-state $[Ca^{2+}]_{ER}$.

Ca^{2+} Induces Autophagy via a Signaling Pathway Involving CaMKK-β and mTOR

Our data show that Ca^{2+} mobilizing agents induce autophagy via a signaling pathway involving CaMKK-β, a Ca^{2+}-activated kinase that was recently identified as a direct activator of AMPK (Hawley et al., 2005; Woods et al., 2005). These data suggest that akin to the other known AMPK kinase, LKB1, that triggers the repression of mTOR under low ATP conditions in an AMPK- and TSC2-dependent manner (Shaw et al., 2004), CaMKK-β may activate a similar pathway in response to an increase in the $[Ca^{2+}]_c$ (Figure 7). The existence of such a pathway is strongly supported by our data showing that CaMKK-β and AMPK are required for the Ca^{2+}-induced autophagosome formation. Furthermore, the Ca^{2+}-induced CaMKK-β-dependent activation of AMPK together with the mounting evidence implicating AMPK in the negative regulation of mTOR points to AMPK-TSC2-RHEB pathway as a possible link between CaMKK-β and autophagy (Sarbassov et al., 2005). It remains to be studied whether CaMKK-β-mediated suppression of mTOR is sufficient to trigger autophagy or whether Ca^{2+} mobilizing agents trigger parallel signaling pathways required for the process.

ER-Localized Bcl-2 Affects Ca^{2+} Handling in the ER and Inhibits Ca^{2+}-Mediated Autophagy

Concordant with our data showing that Bcl-2 has to locate to the ER membrane in order to inhibit EB1089- and ATP-induced autophagy, Levine and coworkers have recently shown that ER-localized, but not mitochondrial, Bcl-2 inhibits starvation-induced autophagy (Pattingre et al., 2005). Based on data suggesting that the autophagy inhibitory effect of Bcl-2 depends on the direct binding of Bcl-2 with Beclin 1, they speculated that the ER-localized Bcl-2-Beclin 1 complex blocks a signal that is essential for the formation of the autophagy promoting Beclin 1-class III PI3K complex. We could, however, not detect any Beclin-1 associated with the ER in untreated MCF-7 cells

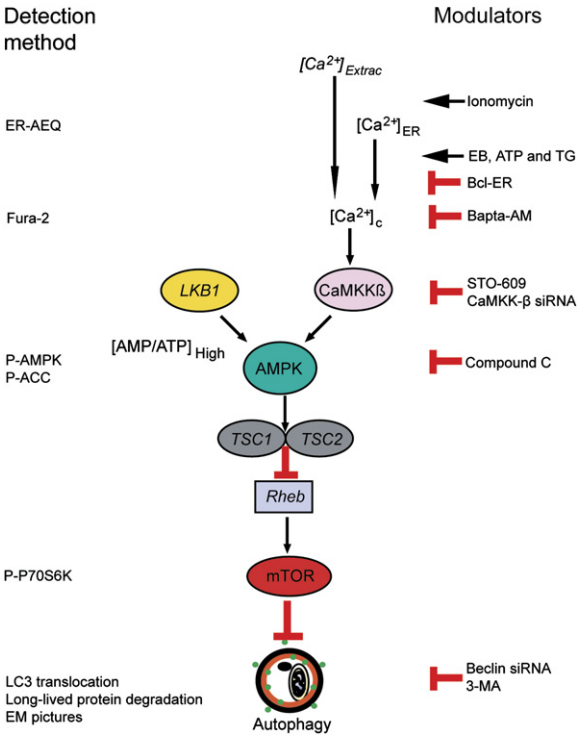

Figure 7. Schematic Presentation of the Suggested Signaling Cascade from the Increase in the $[Ca^{2+}]_c$ to Autophagy

The cartoon in the middle lineates the suggested signaling cascade leading from the increase in the free intracellular Ca^{2+} to increased autophagy. The left and right panels indicate detection methods and tools used in this study to analyze and modulate the indicated events, respectively. The signaling molecules in italics were not studied in this work. For references see the text.

or in cells treated with EB1089 or ionomycin. Instead, we found Beclin 1 in granular dots throughout the cytosol in control cells as well as in cells expressing ectopic Bcl-ER or Beclin 1 (Figure S3). Furthermore, expression of ectopic Beclin 1 in MCF- 7 cells did not have any effect on steady-state $[Ca^{2+}]_{ER}$ or ATP-induced increase in $[Ca^{2+}]_c$ (data not shown). Thus, our data suggest that ER-located Bcl-2 inhibits autophagy induced by Ca^{2+} mobilizing agents by regulating the Ca^{2+} homeostasis in a Beclin 1-independent manner. If the antiautophagy function of Bcl-2 was solely mediated by its effect on the steady-state $[Ca^{2+}]_{ER}$, wild-type Bcl-2 should confer at least partial protection against EB1089- and ATP-induced autophagy in MCF-7 cells. This was, however, not the case. Instead, the ability of the Bcl-2 mutants to inhibit autophagy correlated with their ability to reduce the amount of agonist-induced Ca^{2+} release from the ER. These results, together with the inhibitory effect of BAPTA/AM and the cytosolic induction of CaMKK-β, strongly argue for the involvement of $[Ca^{2+}]_c$ changes in the autophagy induction.

The effect of Bcl-2 on the $[Ca^{2+}]_{ER}$ is controversial, and the literature contains conflicting data showing both increased and decreased $[Ca^{2+}]_{ER}$ in Bcl-2 expressing cells,

depending on the cell type and the methods used (Annis et al., 2004; Ferrari et al., 2002; Oakes et al., 2006). The studies in which $[Ca^{2+}]_{ER}$ has been measured directly by ER-targeted Ca^{2+}-sensitive photoproteins support the view that Bcl-2 mainly acts on $[Ca^{2+}]_{ER}$ by increasing the Ca^{2+} permeability of the ER membrane (Foyouzi-Youssefi et al., 2000; Pinton et al., 2000; Vanden Abeele et al., 2002). Consistent with this view that is compatible with Bcl-2 functioning as an ion channel or a modulator of an ion channel, Bcl-2 reduced the steady-state $[Ca^{2+}]_{ER}$ in the MCF-7 cells. This effect was even more prominent in cells expressing ER-located Bcl-2 and absent if Bcl-2 was targeted to mitochondrial membranes or cytosol, suggesting that Bcl-2 has to physically interact with the ER in order to reduce the $[Ca^{2+}]_{ER}$. Indeed, recent work put forward a potential mechanism to explain the effect of Bcl-2 family members on $[Ca^{2+}]_{ER}$, including their direct interaction with and phosphorylation of the ER resident Ca^{2+} release channel IP_3R (Pinton and Rizzuto, 2006). Along these lines, we cannot exclude that direct interaction of Bcl-ER with ER membrane protein complexes may provide a mechanism to regulate autophagosome formation, which may function parallel to $[Ca^{2+}]_c$ regulation of CaMKK-β, described in this work.

Surprisingly, Bcl-mito enhanced the EB1089-induced depletion of $[Ca^{2+}]_{ER}$. Even though we do not have direct data to explain this phenomenon, two observations may provide some clue. First, ER stress, which is induced by lowering the $[Ca^{2+}]_{ER}$, augments the colocalization of the ER and mitochondrial networks, rendering Bcl-mito in physical contact with the ER (M. Chami, B. Oules, G.S., and P. Paterlini-Brechot, unpublished data). Second, the EM images show that EB1089-treated Bcl-mito cells have significantly more dark electron-dense precipitates in their autophagosome-surrounded mitochondria (Figure 5A). Similar precipitates appear after vast Ca^{2+} load into mitochondria (Pasquali-Ronchetti et al., 1969), suggesting that Ca^{2+} released by EB1089 in Bcl-mito expressing cells is preferentially transported to the mitochondrial matrix. Consequently, this Ca^{2+} load may induce mitochondrial stress and thereby enhance autophagy. In conclusion, by localizing to ER and mitochondria, respectively, Bcl-2 might inhibit the autophagy response by lowering the amount of free ER Ca^{2+} available for release and increase it via the enhanced mitochondrial uptake of Ca^{2+}. Such a combined anti- and proautophagy function of Bcl-2 may help to maintain autophagy at a level that is compatible with cell survival, rather than death.

EXPERIMENTAL PROCEDURES

Cell Culture and Treatments

The MCF-7S1 breast carcinoma and HeLa cell cervix carcinoma cells were cultured in RPMI 1640 with Glutamax (Life Technologies) supplemented with 6% heat-inactivated fetal calf serum (FCS, Biological Industries) and antibiotics. NIH3T3 murine embryonic fibroblasts were grown in D-MEM (Life Technologies) with 10% heat-inactivated FCS and 0.1 mmol/L nonessential amino acids (Invitrogen). MCF10A breast epithelial cells expressing an ecotropic receptor were kindly provided by Dr. Joan Brugge and D. Lynch (Harvard Medical School, Boston, MA, USA) and grown in DMEM-F12 (Life Technologies) with 10% heat-inactivated horse serum, 10 μg/ml insulin, 20 ng/ml epidermal growth factor, 100 ng/mL choleratoxin, 500 ng/ml hydrochortisone, and antibiotics.

EB1089 and 1,25-dihydroxyvitamin D_3 were kindly provided by Lise Binderup (LEO Pharmaceuticals) and human TNF by Anthony Cerami (Kenneth Warren Laboratories, Tarrytown, NY, USA). Ionomycin, TG, and 3-MA were purchased from Sigma-Aldrich (St. Louis, MO), BAPTA/AM and compound C from Calbiochem, and STO-609 from Tocris Bioscience.

Transfections

Plasmids containing cDNAs for wild-type Bcl-2 and its organelle-specific mutants were kindly provided by B. Leber and D.W. Andrews (McMaster University, Hamilton, Ontario, Canada) and subcloned into the episomal vector pCEP4 (Invitrogen). Rat LC3 inserted into pEGFP-C1 (Clontech) and pBabe-puro vectors was a generous gift from G. Kroemer. The plasmid encoding ER-AEQ was described previously (Pinton et al., 2000). Cells were transfected by electroporation essentially as described before (Jäättelä et al., 1995) with Fugene HD (Roche) according to the manufacturer's instructions. MCF10A-EcoR cells were infected with indicated retrovira as previously described (Fehrenbacher et al., 2004).

SiRNAs corresponding to the human cDNA sequence for beclin-1 (5′-CAGTTTGGCACAATCAATA-3′) and a control siRNA (5′-CGACC GAGACAAGCGCAAG-3′) were from Dharmacon Research, for ATG7 (5′-CAGUGGAUCUAAAUCUCAAACUGAU-3′) from Invitrogen, and for CaMKK-α (5′-GGAAGCUUUCCCUACAGGAtt-3′) and CaMKK-β (5′-GGAUCUGAUCAAAGGCAUCtt-3′) from Ambion. MCF-7 and HeLa cells were transfected with 50 and 25 nM siRNA, respectively, employing oligofectamine (Invitrogen).

Autophagy and Apoptosis Detection

Percentages of cells with eGFP-LC3 translocation into dots (a minimum of 100 cells/sample) were counted in eGFP-LC3 expressing cells fixed in 3.7% formaldehyde and 0.19% picric acid (vol/vol) applying Zeiss Axiovert 100 M Confocal Laser Scanning Microscope.

Protein degradation and transmission EM were evaluated as described previously (Høyer-Hansen et al., 2005). For quantifying autophagic cells in EM images, a minimum of 30 cells was counted in each sample.

Cell death was analyzed by determining DNA fragmentation (cytosolic histone-bound DNA) employing the Cell Death Detection ELISAplus kit (Roche) or by flow cytometry (Becton Dickinson, San Jose, CA) of cells stained with SYTOX Green (S-7020, Molecular Probes) as described previously (Høyer-Hansen et al., 2005).

Immunodetection

The primary antibodies used for immunoblot analysis included murine antibodies against Bcl-2 (clone 124, Boehringer Mannheim), Beclin 1 (clone 20, BD Transduction Laboratories), GAPDH (Biogenesis), and p-$p70^{S6K}$ (Thr389) (#9206, Cell Signaling Technology, Inc, Danvers, MA); rabbit antibodies against $p70^{S6K}$ (#9202), AMPK (#2630), and p-AMPK (#2535) from Cell Signaling Technology; Atg7 from ProSci Incorporated (Poway, CA, USA; #3617); and p-ACC (#07-303) from Upstate and Hsc70 from StressGen. The appropriate peroxidase-conjugated secondary antibodies were from DAKO A/S and ECL immunoblotting reagents from Amersham Biosciences. The IMAGEJ and IMAGE GAUGE (Fuji) densitometry software was used to quantify the proteins level.

For immunocytochemistry, the cells were fixed with 3.7% formaldehyde and permeabilized in 0.2% Triton X-100. After blocking in 5% donkey or goat serum, the slides were incubated with murine antibodies against cytochrome *c* (clone 6H2.B4 form Pharmigen), SERCA (Calbiochem), and Beclin 1 (clone 20, BD Transduction Laboratories) as well as rabbit anti-Bcl-2 (Stressgen). The appropriate fluorescent

secondary antibodies were from Molecular Probes. Pictures were taken with a Confocal Laser Scanning Microscope (Zeiss Axiovert 100M equipped with LSM510 system).

RT-PCR

The quantitative RT-PCR using porphobilinogen deaminase (PBDG) as an internal control was preformed essentially as described (Rohde et al., 2005). The following primers were applied: CaMKK-α, 5′-GACATCAAGCCATCCAACCT-3′ and 5′-GGGCACTTCCCATAGACA AA-3′; CaMKK-β, 5′-AGACCAGGCCCGTTTCTACT-3′ and 5′-GAA GATCTTGCGGGTCTCAG-3′.

Dynamic In Vivo $[Ca^{2+}]$ Measurements with Targeted Aequorin Probes and fura-2

For $[Ca^{2+}]_{ER}$ measurements, ER-AEQ-transfected cells were reconstituted with coelenterazine after ER Ca^{2+} depletion in a solution containing $[Ca^{2+}]$, 600 μM EGTA, and 1 μM ionomycin, as described (Szabadkai et al., 2004). Cells were transferred to the perfusion chamber, and light signal was collected in a purpose-built luminometer and calibrated into $[Ca^{2+}]$ values (Chiesa et al., 2001). All aequorin measurements were carried out in KRB containing 1 mM $CaCl_2$ (KRB/Ca^{2+}, Krebs-Ringer modified buffer: 135 mM NaCl, 5 mM KCl, 1 mM $MgSO_4$, 0.4 mM K_2HPO_4, 1 mM $CaCl_2$, 5.5 mM glucose, and 20 mM HEPES [pH 7.4]). Kinetic imaging of $[Ca^{2+}]_c$ transients in fura-2-loaded cells was performed as previously described (Szabadkai et al., 2004).

Statistical Analysis

Independent experiments were pooled when the coefficient of variance could be assumed identical. Statistical significance was evaluated by using one or two sample t tests. A p value of less than 0.05 was considered significant.

Supplemental Data

Supplemental Data include three figures and can be found with this article online at http://www.molecule.org/cgi/content/full/25/2/193/DC1/.

ACKNOWLEDGMENTS

We thank K. Grøn Henriksen, J. Hinrichsen, T. Chabaan, and D. Czerny for excellent technical assistance and D. Andrews, L. Binderup, J. Brugge, A. Cerami, G. Kroemer, B. Leber, D. Lynch, and B. Levine for invaluable research tools. This work was supported by grants from the Danish Cancer Society, Danish Medical Research Council, Danish National Research Foundation, and Meyer Foundation to M.J., the Association for International Cancer Research to M.J. and R.R., the Novo Nordisk Foundation to M.J. and M.H.H., and the Telethon-Italy, Italian University Ministry (PRIN, FIRB, and local research grants), Emilia-Romagna PRRIITT program, and Italian Space Agency (ASI) to R.R.

Received: August 3, 2006
Revised: November 2, 2006
Accepted: December 11, 2006
Published: January 25, 2007

REFERENCES

Annis, M.G., Yethon, J.A., Leber, B., and Andrews, D.W. (2004). There is more to life and death than mitochondria: Bcl-2 proteins at the endoplasmic reticulum. Biochim. Biophys. Acta *1644*, 115–123.

Baehrecke, E.H. (2005). Autophagy: dual roles in life and death? Nat. Rev. Mol. Cell Biol. *6*, 505–510.

Chiesa, A., Rapizzi, E., Tosello, V., Pinton, P., de Virgilio, M., Fogarty, K.E., and Rizzuto, R. (2001). Recombinant aequorin and green fluorescent protein as valuable tools in the study of cell signalling. Biochem. J. *355*, 1–12.

Codogno, P., and Meijer, A.J. (2005). Autophagy and signaling: their role in cell survival and cell death. Cell Death Differ. *12* (*Suppl 2*), 1509–1518.

Dixon, C.J., Bowler, W.B., Fleetwood, P., Ginty, A.F., Gallagher, J.A., and Carron, J.A. (1997). Extracellular nucleotides stimulate proliferation in MCF-7 breast cancer cells via P2-purinoceptors. Br. J. Cancer *75*, 34–39.

Fehrenbacher, N., Gyrd-Hansen, M., Poulsen, B., Felbor, U., Kallunki, T., Boes, M., Weber, E., Leist, M., and Jäättelä, M. (2004). Sensitization to the lysosomal cell death pathway upon immortalization and transformation. Cancer Res. *64*, 5301–5310.

Ferrari, D., Pinton, P., Szabadkai, G., Chami, M., Campanella, M., Pozzan, T., and Rizzuto, R. (2002). Endoplasmic reticulum, Bcl-2 and Ca2+ handling in apoptosis. Cell Calcium *32*, 413–420.

Foyouzi-Youssefi, R., Arnaudeau, S., Borner, C., Kelley, W.L., Tschopp, J., Lew, D.P., Demaurex, N., and Krause, K.H. (2000). Bcl-2 decreases the free Ca2+ concentration within the endoplasmic reticulum. Proc. Natl. Acad. Sci. USA *97*, 5723–5728.

Gordon, P.B., Holen, I., Fosse, M., Rotnes, J.S., and Seglen, P.O. (1993). Dependence of hepatocytic autophagy on intracellularly sequestered calcium. J. Biol. Chem. *268*, 26107–26112.

Hara, T., Nakamura, K., Matsui, M., Yamamoto, A., Nakahara, Y., Suzuki-Migishima, R., Yokoyama, M., Mishima, K., Saito, I., Okano, H., and Mizushima, N. (2006). Suppression of basal autophagy in neural cells causes neurodegenerative disease in mice. Nature *441*, 885–889.

Hawley, S.A., Pan, D.A., Mustard, K.J., Ross, L., Bain, J., Edelman, A.M., Frenguelli, B.G., and Hardie, D.G. (2005). Calmodulin-dependent protein kinase kinase-beta is an alternative upstream kinase for AMP-activated protein kinase. Cell Metab. *2*, 9–19.

Høyer-Hansen, M., Bastholm, L., Mathiasen, I.S., Elling, F., and Jäättelä, M. (2005). Vitamin D analog EB1089 triggers dramatic lysosomal changes and Beclin 1-mediated autophagic cell death. Cell Death Differ. *12*, 1297–1309.

Jäättelä, M., Benedict, M., Tewari, M., Shayman, J.A., and Dixit, V.M. (1995). Bcl-x and Bcl-2 inhibit TNF and Fas-induced apoptosis and activation of phospholipase A_2 in breast carcinoma cells. Oncogene *10*, 2297–2305.

Kao, J.P. (1994). Practical aspects of measuring [Ca2+] with fluorescent indicators. Methods Cell Biol. *40*, 155–181.

Klionsky, D.J., Cregg, J.M., Dunn, W.A., Jr., Emr, S.D., Sakai, Y., Sandoval, I.V., Sibirny, A., Subramani, S., Thumm, M., Veenhuis, M., and Ohsumi, Y. (2003). A unified nomenclature for yeast autophagy-related genes. Dev. Cell *5*, 539–545.

Komatsu, M., Waguri, S., Chiba, T., Murata, S., Iwata, J.I., Tanida, I., Ueno, T., Koike, M., Uchiyama, Y., Kominami, E., and Tanaka, K. (2006). Loss of autophagy in the central nervous system causes neurodegeneration in mice. Nature *441*, 880–884.

Kroemer, G., and Jäättelä, M. (2005). Lysosomes and autophagy in cell death control. Nat. Rev. Cancer *5*, 886–897.

Levine, B., and Klionsky, D.J. (2004). Development by self-digestion: molecular mechanisms and biological functions of autophagy. Dev. Cell *6*, 463–477.

Lum, J.J., Bauer, D.E., Kong, M., Harris, M.H., Li, C., Lindsten, T., and Thompson, C.B. (2005). Growth factor regulation of autophagy and cell survival in the absence of apoptosis. Cell *120*, 237–248.

Mathiasen, I.S., Sergeev, I.N., Bastholm, L., Elling, F., Norman, A.W., and Jäättelä, M. (2002). Calcium and calpain as key mediators of apoptosis-like death induced by vitamin D compounds in breast cancer cells. J. Biol. Chem. *277*, 30738–30745.

Oakes, S.A., Scorrano, L., Opferman, J.T., Bassik, M.C., Nishino, M., Pozzan, T., and Korsmeyer, S.J. (2005). Proapoptotic BAX and BAK

regulate the type 1 inositol trisphosphate receptor and calcium leak from the endoplasmic reticulum. Proc. Natl. Acad. Sci. USA *102*, 105–110.

Oakes, S.A., Lin, S.S., and Bassik, M.C. (2006). The control of endoplasmic reticulum-initiated apoptosis by the BCL-2 family of proteins. Curr. Mol. Med. *6*, 99–109.

Onodera, J., and Ohsumi, Y. (2005). Autophagy is required for maintenance of amino acid levels and protein synthesis under nitrogen starvation. J. Biol. Chem. *280*, 31582–31586.

Pasquali-Ronchetti, I., Greenawalt, J.W., and Carafoli, E. (1969). On the nature of the dense matrix granules of normal mitochondria. J. Cell Biol. *40*, 565–568.

Pattingre, S., Tassa, A., Qu, X., Garuti, R., Liang, X.H., Mizushima, N., Packer, M., Schneider, M.D., and Levine, B. (2005). Bcl-2 antiapoptotic proteins inhibit Beclin 1-dependent autophagy. Cell *122*, 927–939.

Pinton, P., and Rizzuto, R. (2006). Bcl-2 and Ca(2+) homeostasis in the endoplasmic reticulum. Cell Death Differ. *13*, 1409–1418.

Pinton, P., Ferrari, D., Magalhaes, P., Schulze-Osthoff, K., Di Virgilio, F., Pozzan, T., and Rizzuto, R. (2000). Reduced loading of intracellular Ca(2+) stores and downregulation of capacitative Ca(2+) influx in Bcl-2-overexpressing cells. J. Cell Biol. *148*, 857–862.

Qu, X., Yu, J., Bhagat, G., Furuya, N., Hibshoosh, H., Troxel, A., Rosen, J., Eskelinen, E.L., Mizushima, N., Ohsumi, Y., et al. (2003). Promotion of tumorigenesis by heterozygous disruption of the beclin 1 autophagy gene. J. Clin. Invest. *112*, 1809–1820.

Ravikumar, B., Vacher, C., Berger, Z., Davies, J.E., Luo, S., Oroz, L.G., Scaravilli, F., Easton, D.F., Duden, R., O'Kane, C.J., and Rubinsztein, D.C. (2004). Inhibition of mTOR induces autophagy and reduces toxicity of polyglutamine expansions in fly and mouse models of Huntington disease. Nat. Genet. *36*, 585–595.

Rohde, M., Daugaard, M., Jensen, M.H., Helin, K., Nylandsted, J., and Jäättelä, M. (2005). Members of the heat-shock protein 70 family promote cancer cell growth by distinct mechanisms. Genes Dev. *19*, 570–582.

Sarbassov, D.D., Ali, S.M., and Sabatini, D.M. (2005). Growing roles for the mTOR pathway. Curr. Opin. Cell Biol. *17*, 596–603.

Shaw, R.J., Bardeesy, N., Manning, B.D., Lopez, L., Kosmatka, M., DePinho, R.A., and Cantley, L.C. (2004). The LKB1 tumor suppressor negatively regulates mTOR signaling. Cancer Cell *6*, 91–99.

Shimizu, S., Kanaseki, T., Mizushima, N., Mizuta, T., Arakawa-Kobayashi, S., Thompson, C.B., and Tsujimoto, Y. (2004). Role of Bcl-2 family proteins in a non-apoptotic programmed cell death dependent on autophagy genes. Nat. Cell Biol. *6*, 1221–1228.

Szabadkai, G., Varnai, P., and Enyedi, P. (1999). Selective inhibition of potassium-stimulated rat adrenal glomerulosa cells by ruthenium red. Biochem. Pharmacol. *57*, 209–218.

Szabadkai, G., Simoni, A.M., Chami, M., Wieckowski, M.R., Youle, R.J., and Rizzuto, R. (2004). Drp-1-dependent division of the mitochondrial network blocks intraorganellar Ca2+ waves and protects against Ca2+-mediated apoptosis. Mol. Cell *16*, 59–68.

Tokumitsu, H., Inuzuka, H., Ishikawa, Y., Ikeda, M., Saji, I., and Kobayashi, R. (2002). STO-609, a specific inhibitor of the Ca(2+)/calmodulin-dependent protein kinase kinase. J. Biol. Chem. *277*, 15813–15818.

Tsujimoto, Y., and Shimizu, S. (2005). Another way to die: autophagic programmed cell death. Cell Death Differ. *12* (*Suppl 2*), 1528–1534.

Vanden Abeele, F., Skryma, R., Shuba, Y., Van Coppenolle, F., Slomianny, C., Roudbaraki, M., Mauroy, B., Wuytack, F., and Prevarskaya, N. (2002). Bcl-2-dependent modulation of Ca(2+) homeostasis and store-operated channels in prostate cancer cells. Cancer Cell *1*, 169–179.

Wang, Z., Wilson, W.A., Fujino, M.A., and Roach, P.J. (2001). Antagonistic controls of autophagy and glycogen accumulation by Snf1p, the yeast homolog of AMP-activated protein kinase, and the cyclin-dependent kinase Pho85p. Mol. Cell. Biol. *21*, 5742–5752.

White, C., Li, C., Yang, J., Petrenko, N.B., Madesh, M., Thompson, C.B., and Foskett, J.K. (2005). The endoplasmic reticulum gateway to apoptosis by Bcl-X(L) modulation of the InsP3R. Nat. Cell Biol. *7*, 1021–1028.

Woods, A., Dickerson, K., Heath, R., Hong, S.P., Momcilovic, M., Johnstone, S.R., Carlson, M., and Carling, D. (2005). Ca2+/calmodulin-dependent protein kinase kinase-beta acts upstream of AMP-activated protein kinase in mammalian cells. Cell Metab. *2*, 21–33.

Yue, Z., Jin, S., Yang, C., Levine, A.J., and Heintz, N. (2003). Beclin *1*, an autophagy gene essential for early embryonic development, is a haploinsufficient tumor suppressor. Proc. Natl. Acad. Sci. USA *100*, 15077–15082.

Zhu, W., Cowie, A., Wasfy, G.W., Penn, L.Z., Leber, B., and Andrews, D.W. (1996). Bcl-2 mutants with restricted subcellular location reveal spatially disinct pathways for apoptosis in different cell types. EMBO J. *15*, 4130–4141.